

# A macroscopic multi-mechanism based constitutive model for the thermo-mechanical cyclic degeneration of shape memory effect of NiTi shape memory alloy

Chao Yu<sup>1,2</sup> · Guozheng Kang<sup>1,2</sup> · Qianhua Kan<sup>2</sup>

Received: 21 July 2016 / Revised: 13 November 2016 / Accepted: 14 December 2016 / Published online: 27 January 2017

© The Chinese Society of Theoretical and Applied Mechanics; Institute of Mechanics, Chinese Academy of Sciences and Springer-Verlag Berlin Heidelberg 2017

**Abstract** A macroscopic based multi-mechanism constitutive model is constructed in the framework of irreversible thermodynamics to describe the degeneration of shape memory effect occurring in the thermo-mechanical cyclic deformation of NiTi shape memory alloys (SMAs). Three phases, austenite  $A$ , twinned martensite  $M^t$  and detwinned martensite  $M^d$ , as well as the phase transitions occurring between each pair of phases ( $A \rightarrow M^t$ ,  $M^t \rightarrow A$ ,  $A \rightarrow M^d$ ,  $M^d \rightarrow A$ , and  $M^t \rightarrow M^d$ ) are considered in the proposed model. Meanwhile, two kinds of inelastic deformation mechanisms, martensite transformation-induced plasticity and reorientation-induced plasticity, are used to explain the degeneration of shape memory effects of NiTi SMAs. The evolution equations of internal variables are proposed by attributing the degeneration of shape memory effect to the interaction between the three phases ( $A$ ,  $M^t$ , and  $M^d$ ) and plastic deformation. Finally, the capability of the proposed model is verified by comparing the predictions with the experimental results of NiTi SMAs. It is shown that the degeneration of shape memory effect and its dependence on the loading level can be reasonably described by the proposed model.

**Keywords** NiTi SMAs · Constitutive model · Cyclic degeneration of shape memory effect · Transformation-induced plasticity · Reorientation-induced plasticity

## 1 Introduction

NiTi shape memory alloys (SMAs) have been used extensively in many engineering fields such as biomedicine, micro-electromechanical systems and aerospace, due to their unique super-elasticity and shape memory effects originating from their solid-solid thermo-elastic martensite transformation and good biological compatibility. In these applications, the structure components and devices of NiTi SMAs are unavoidably subjected to a thermo-mechanical cyclic loading. So, the cyclic deformation of NiTi SMAs and its constitutive model are key issues in assessing the fatigue life and reliability of such components and devices.

In the last three decades, the degeneration of super-elasticity of NiTi SMAs under pure mechanical loading conditions and at temperatures higher than the finish temperature of austenite  $A_f$  have been investigated by many experimental observations. It was reported that the degeneration of super-elasticity occurred during the cyclic deformation of NiTi SMAs. That is, the residual strain occurred and progressively accumulated; the start stress of martensite transformation and the dissipation energy (i.e., the area of the stress-strain hysteresis loop per cycle) decreased, but the transformation hardening increased with the increasing number of cycles, accompanied with the repeated martensite transformation and its reverse [1]. All of these physical variables would tend to be saturated after certain numbers of cycles. The degeneration of super-elasticity was further investigated with more

✉ Guozheng Kang  
guozhengkang@home.swjtu.edu.cn;  
guozhengkang@126.com

<sup>1</sup> State Key Laboratory of Traction Power, Southwest Jiaotong University, Chengdu 610031, China

<sup>2</sup> Applied Mechanics and Structure Safety Key Laboratory of Sichuan Province, School of Mechanics and Engineering, Southwest Jiaotong University, Chengdu 610031, China

factors considered, including the loading paths [2,3], loading rate [4,5], grain size [6], and so on.

Recently, the degeneration of shape memory effect was observed by Kan et al. [7] in the thermo-mechanical cyclic deformation of NiTi SMA. During the thermo-mechanical cyclic loading (e.g., in the repeated loading–unloading–heating–cooling process), it was observed that the degeneration of shape memory effect occurred, i.e., the residual/peak strains accumulated, the martensite reorientation and transformation hardening moduli increased, but the start stress of martensite reorientation, start temperature of reverse transformation and the hysteresis loops presented in the stress-strain and temperature-strain curves decreased with the increasing number of cycles. Meanwhile, additional inelastic deformation occurred in the cooling stage of each thermo-mechanical cycle and increased with the increasing number of cycles. Furthermore, the degeneration of shape memory effect depended strongly on the loading level, and became more and more apparent with the increasing loading level.

On the theoretical aspect, two main approaches are used to describe the solid-solid phase transformation phenomena of SMAs. The first approach treats the phase transformation as a multiscale process. It aims to establish a direct link between the macroscopic phenomena and underlying events at different length and time scales [8–14], which is very useful for understanding the physics of martensite transformation. The second approach considers the martensite transformation to be a macroscopic phenomenological process, and constructs constitutive models directly from experimental observations. Owing to their low computational cost, the macroscopic phenomenological constitutive models are very suitable for engineering applications after they are implemented into the finite element codes. In the last two decades, many macroscopic constitutive models have been constructed to describe the thermo-mechanical cyclic deformation of NiTi SMAs. The representative works can be referred to [15–21]. The degeneration of super-elasticity occurring in the cyclic deformation of super-elastic NiTi SMAs can be reasonably described by these models. However, due to the lack of experimental data, the capability of these models in describing the cyclic degeneration of shape memory effect has not yet been verified. Recently, a physical mechanism-based crystal plasticity model was constructed by Yu et al. [22] to address the degeneration of shape memory effect occurring in the cyclic deformation of the NiTi SMAs. The model considered 24 martensite variants and relative slipping systems in the scale of a single crystal. Different mechanisms of inelastic deformation, including the martensite transformation and reorientation, the transformation-induced and reorientation-induced plasticity and their interaction, were taken into account. Although the crystal plasticity-based models can represent the microstructure information well,

they are not suitable for structural analysis of NiTi SMA engineering components and devices due to their high computational cost.

Therefore, a macroscopic constitutive model is constructed in this work to describe the degeneration of shape memory effect occurring in the cyclic deformation of NiTi SMAs. In Sect. 2, based on the framework of irreversible thermodynamics, the construction of macroscopic multi-mechanism-based constitutive model is introduced. Two mechanisms of inelastic deformation related to the degeneration of shape memory effect, martensite transformation-induced and reorientation-induced plasticity are addressed. In Sect. 3, the determination procedures of material parameters used in the proposed model are discussed. In Sect. 4, the capability of the proposed model to describe the thermo-mechanical cyclic degeneration of the shape memory effect of NiTi SMA is verified by comparing the predicted results with the corresponding experimental results obtained by Kan et al. [7].

## 2 Constitutive model

### 2.1 Physical mechanism for the degeneration of shape memory effect

Following Popov and Lagoudas [23], we introduce three phases, austenite  $A$ , twinned martensite  $M^t$ , and detwinned martensite  $M^d$ , to characterize the states of the NiTi SMAs. These phases and the phase transitions occurring between each pair of them are illustrated in Fig. 1. The volume fractions of the phases  $A$ ,  $M^t$ , and  $M^d$  are denoted as  $\xi_A$ ,  $\xi_M^t$ , and  $\xi_M^d$ , respectively. In order to describe the phase transitions shown in Fig. 1, three internal variables  $\lambda_1$ ,  $\lambda_2$ , and  $\lambda_3$  are introduced by referring to Popov and Lagoudas [23]:

$$\begin{aligned} \lambda_1: \xi_A &\leftrightarrow \xi_M^t, \\ \lambda_2: \xi_A &\leftrightarrow \xi_M^d, \\ \lambda_3: \xi_M^t &\rightarrow \xi_M^d, \quad \dot{\lambda}_3 \geq 0, \end{aligned} \quad (1)$$

where  $\lambda_1$ ,  $\lambda_2$ , and  $\lambda_3$  represent the amount of phase transition from the austenite to twinned martensite, the austenite to detwinned martensite and the twinned martensite to detwinned martensite phase, respectively. It should be noted the rate of  $\lambda_3$  should be non-negative, i.e.,  $\dot{\lambda}_3 \geq 0$ , since the transformation from the detwinned to twinned martensite phase is not thermodynamically stable [23]. In this work, the martensite transformation means the phase transition from the austenite to twinned or detwinned martensite phase, and the martensite reorientation implies the phase transition from the twinned martensite to detwinned martensite phase. The amount of phase transitions,  $\lambda_1$ ,  $\lambda_2$ , and  $\lambda_3$  can be connected

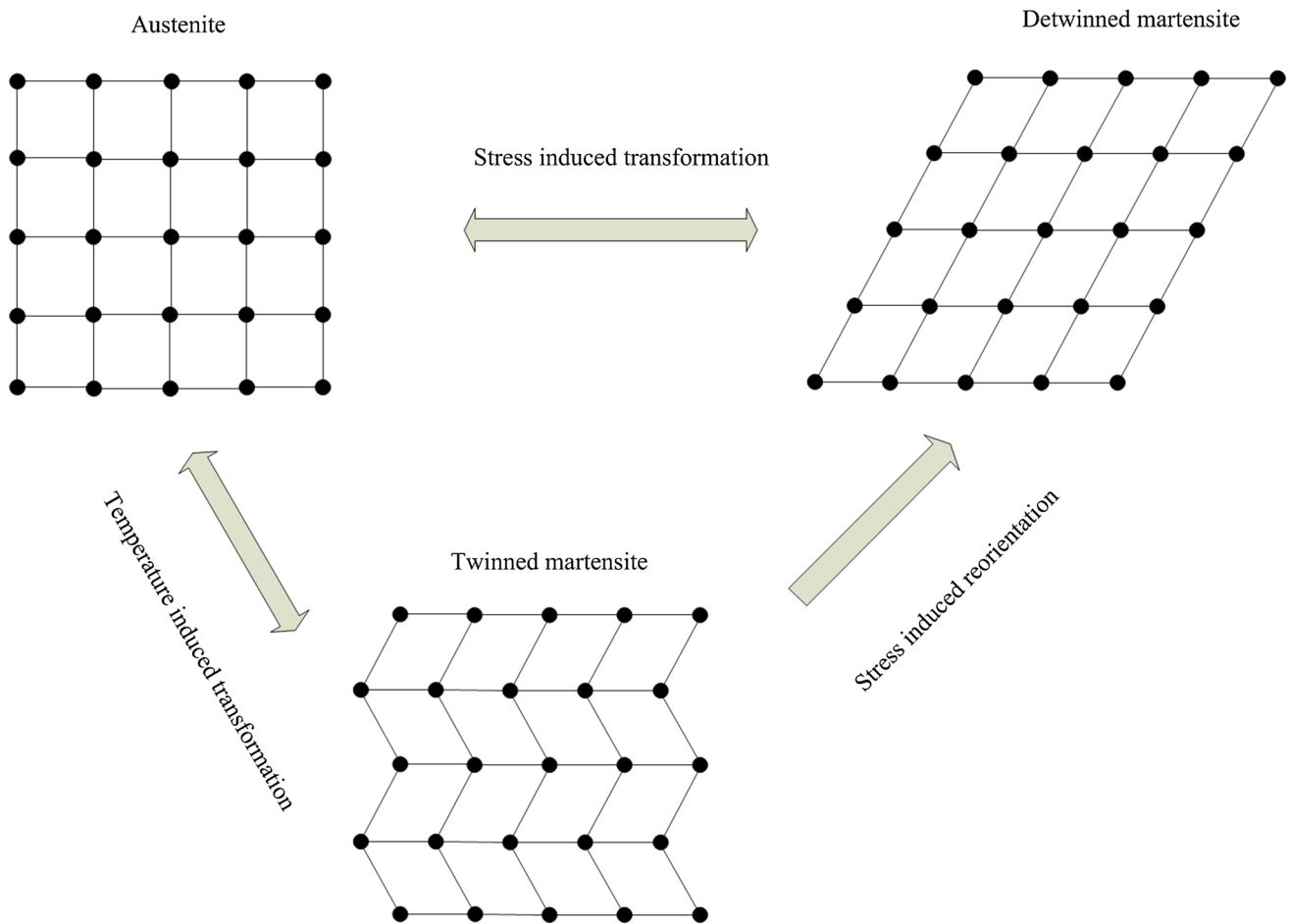


**Fig. 1** Austenite, twinned martensite, detwinned martensite, and the phase transitions between every two of them

to the three volume fractions by:

$$\xi_A = \xi_A^0 - \lambda_1 - \lambda_2, \tag{2a}$$

$$\xi_M^t = \xi_M^{t0} + \lambda_1 - \lambda_3, \tag{2b}$$

$$\xi_M^d = \xi_M^{d0} + \lambda_2 + \lambda_3, \tag{2c}$$

where  $\xi_A^0$ ,  $\xi_M^{t0}$ , and  $\xi_M^{d0}$  are the initial values of  $\xi_A$ ,  $\xi_M^t$ , and  $\xi_M^d$ , respectively. The values of  $\xi_A^0$ ,  $\xi_M^{t0}$ ,  $\xi_M^{d0}$ ,  $\xi_A$ ,  $\xi_M^t$ , and  $\xi_M^d$  are constrained by the following conditions

$$\xi_A^0 + \xi_M^{t0} + \xi_M^{d0} = 1, \tag{3a}$$

$$\xi_A + \xi_M^t + \xi_M^d = 1, \tag{3b}$$

$$0 \leq \xi_A^0 \leq 1, \quad 0 \leq \xi_M^{t0} \leq 1, \quad 0 \leq \xi_M^{d0} \leq 1, \tag{3c}$$

$$0 \leq \xi_A \leq 1, \quad 0 \leq \xi_M^t \leq 1, \quad 0 \leq \xi_M^d \leq 1. \tag{3d}$$

Before the construction of our constitutive model, we will explain the physical mechanism for the degeneration of shape memory effect by the evolution of the three phases just introduced.

Figure 2 illustrates a typical stress-strain-temperature curve of shape memory NiTi SMA from experimental obser-

vations [7], obtained in the first thermo-mechanical cycle and corresponding variation of three phases ( $A$ ,  $M^t$ , and  $M^d$ ).

Before the cyclic deformation, the original phase of the NiTi SMA is the twinned martensite phase, since the test temperature is lower than the finish temperature of martensite  $M_f$ , and is assumed to be defect-free from point o to point a shown in Fig. 2. When the applied stress reaches a critical value, martensite reorientation occurs. In the subsequent deformation process (i.e., from point a to point b shown in Fig. 2), the domain of detwinned martensite expands but that of twinned martensite shrinks gradually, which results in a reorientation strain. Meanwhile, dislocation slipping is induced in the process of martensite reorientation; such an inelastic deformation mechanism is named as reorientation-induced plasticity by Yu et al. [24]. When the martensite reorientation becomes completed (i.e., at point b), the NiTi SMA consists of the detwinned martensite phase with some dislocations as shown in Fig. 2. In the next loading or unloading, only an elastic deformation of the detwinned martensite phase occurs. In the process of heating, when the temperature reaches a critical value, reverse transformation (from the

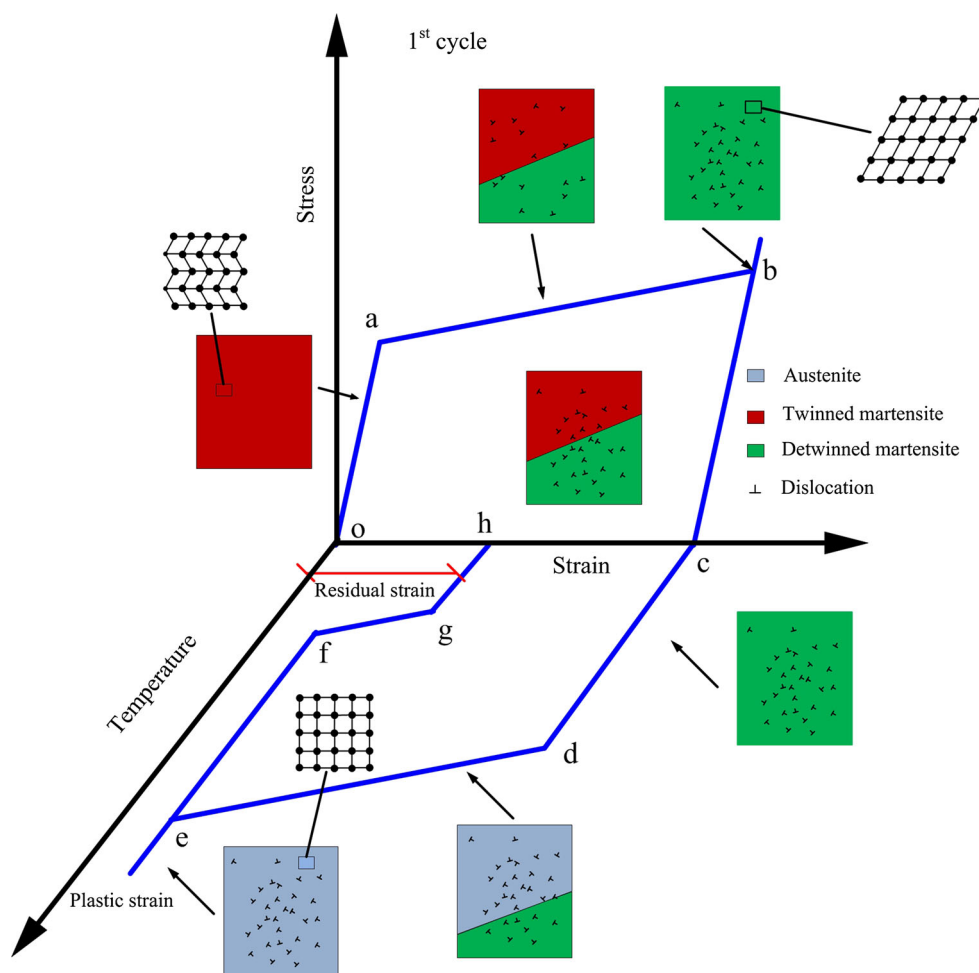


**Fig. 2** (Color online) Illustration for the cyclic degeneration of shape memory effect and the evolutions of three phases (i.e., austenite, twinned martensite, and detwinned martensite) in the NiTi SMA (where initial phase is twinned martensite)

detwinned martensite to the austenite phase) occurs, and the domain of detwinned martensite shrinks with the increasing temperature (i.e., from point d to point e in Fig. 2). Also, the dislocation slippage is caused by the martensite transformation; such an inelastic deformation mechanism is called transformation-induced plasticity [25,26]. When the temperature is high enough (i.e., at point e), the detwinned martensite phase disappears completely, but an amount of dislocations are left in the austenite phase as shown in Fig. 2. It should be noted that, although the reverse transformation is pinned by the dislocations [27], the detwinned martensite can be transformed completely into the austenite phase if the temperature is high enough [28]. Thus, the accumulated inelastic strain at point e only comes from the dislocation slippage, and is called a plastic strain.

During the subsequent cooling, a self-balanced internal stress caused by dislocations exists in the NiTi SMA. The martensite transformation can be induced by stress (resulting in detwinned martensite) and temperature (resulting in

twinned martensite). However, owing to the existing internal stress, the twinned and detwinned martensite phases can be simultaneously formed, even if the applied stress is zero. Then, a new inelastic strain (i.e., at point g) occurs during the cooling process. This implies that the accumulated inelastic strain occurring at point g comes from the dislocation slippage and martensite transformation strain, simultaneously, which is called a residual strain.

During the thermo-mechanical cyclic degeneration of shape memory effect, the increased transformation and reorientation moduli, the start temperature of martensite transformation, and the decreased start stress of martensite reorientation can be explained by the local stress and stress gradient [1]. At the beginning of the  $n$ -th ( $n \geq 0$ ) cycle, in some regions, the projection of the local stress tensor caused by the dislocations on the applied stress tensor is positive, which can prompt the martensite transformation and reorientation. Thus, the start stress of martensite reorientation decreases, but the start temperature of martensite transfor-

mation increases during the cyclic deformation. Meanwhile, a stress gradient caused by the dislocations can hinder the growth of the twinned and detwinned martensite phases, and cause a progressive increase in the martensite transformation and reorientation moduli during the cyclic loading.

### 2.2 Definitions of inelastic strains

Based on the hypothesis of small deformation, the total strain tensor  $\boldsymbol{\epsilon}$  in a material point is decomposed into five parts: elastic strain  $\boldsymbol{\epsilon}^e$ , transformation strain  $\boldsymbol{\epsilon}^{tr}$ , reorientation strain  $\boldsymbol{\epsilon}^{reo}$ , transformation-induced plastic strain  $\boldsymbol{\epsilon}^{tp}$ , and reorientation-induced plastic strain tensors  $\boldsymbol{\epsilon}^{rp}$ . This yields:

$$\boldsymbol{\epsilon} = \boldsymbol{\epsilon}^e + \boldsymbol{\epsilon}^{in}, \tag{4a}$$

$$\boldsymbol{\epsilon}^{in} = \boldsymbol{\epsilon}^{tr} + \boldsymbol{\epsilon}^{reo} + \boldsymbol{\epsilon}^{tp} + \boldsymbol{\epsilon}^{rp}, \tag{4b}$$

where  $\dot{\boldsymbol{\epsilon}}^{in}$  is the inelastic strain tensor.

The relation between the transformation strain rate  $\dot{\boldsymbol{\epsilon}}^{tr}$  and the rate of transition amount  $\dot{\lambda}_2$  can be formulated as follows

$$\dot{\boldsymbol{\epsilon}}^{tr} = g N_{tr} \dot{\lambda}_2, \tag{5a}$$

$$N_{tr} = \begin{cases} \sqrt{\frac{3}{2}} \frac{\boldsymbol{\sigma}_{dev} + \mathbf{B}_{tr}}{\|\boldsymbol{\sigma}_{dev} + \mathbf{B}_{tr}\|}, & \dot{\lambda}_2 > 0, \\ \sqrt{\frac{3}{2}} \frac{\boldsymbol{\epsilon}^{tr} + \boldsymbol{\epsilon}^{reo}}{\|\boldsymbol{\epsilon}^{tr} + \boldsymbol{\epsilon}^{reo}\|}, & \dot{\lambda}_2 < 0, \end{cases} \tag{5b}$$

where  $g$  is the magnitude of transformation strain generated in a full forward transformation,  $N_{tr}$  is the direction tensor of martensite transformation,  $\boldsymbol{\sigma}_{dev}$  is the deviator of stress tensor  $\boldsymbol{\sigma}$ , and  $\mathbf{B}_{tr}$  is the internal stress related to the martensite transformation.

The relation between the reorientation strain rate  $\dot{\boldsymbol{\epsilon}}^{reo}$  and the rate of transition amount  $\dot{\lambda}_3$  can be given as

$$\dot{\boldsymbol{\epsilon}}^{reo} = g N_{reo} \dot{\lambda}_3, \tag{6a}$$

$$N_{reo} = \sqrt{\frac{3}{2}} \frac{\boldsymbol{\sigma}_{dev} + \mathbf{B}_{reo}}{\|\boldsymbol{\sigma}_{dev} + \mathbf{B}_{reo}\|}, \tag{6b}$$

where  $N_{reo}$  is the direction tensor of martensite reorientation and  $\mathbf{B}_{reo}$  is the internal stress related to the martensite reorientation.

The transformation-induced and reorientation-induced plastic strains are written as

$$\dot{\boldsymbol{\epsilon}}^{tp} = N_{tr} \dot{\gamma}_{tp}, \tag{7a}$$

$$\dot{\boldsymbol{\epsilon}}^{rp} = N_{reo} \dot{\gamma}_{rp}, \tag{7b}$$

where  $\dot{\gamma}_{tp}$  and  $\dot{\gamma}_{rp}$  are, respectively, the slipping rates related to the transformation-induced and reorientation-induced plasticity.

### 2.3 The framework of thermodynamics

In the framework of continuum thermodynamics, Helmholtz's free energy at a material point can be written as

$$\psi = \psi^e + \psi^T + \psi^{int} + \psi_M^h + \psi_p^h, \tag{8}$$

where  $\psi^e$  is the elastic energy of the representative volume element (RVE),  $\psi^{int}$  is an additional energy caused by the internal stress,  $\psi^T$  is the energy related to the temperature,  $\psi_M^h$  is the hardening energy caused by the martensite transformation and reorientation, and  $\psi_p^h$  is the hardening energy caused by the transformation-induced and reorientation-induced plasticity. The explicit expression of each term in the Helmholtz free energy can be given as

$$\psi^e(\boldsymbol{\epsilon}^e) = \frac{1}{2} \boldsymbol{\epsilon}^e : \mathbf{C} : \boldsymbol{\epsilon}^e, \tag{9a}$$

$$\psi^T(T, \lambda_1, \lambda_2) = c \left[ (T - T_0) - T \ln \left( \frac{T}{T_0} \right) \right] - F_1(T) \lambda_1 - F_2(T) \lambda_2, \tag{9b}$$

$$\psi^{int} = - \int_0^t \left( \mathbf{B}_{tr} : \frac{d\boldsymbol{\epsilon}^{tr}}{d\tau} + \mathbf{B}_{reo} : \frac{d\boldsymbol{\epsilon}^{reo}}{d\tau} \right) d\tau, \tag{9c}$$

$$\psi_M^h = \int_0^t \left( f_1 \frac{d\lambda_1}{d\tau} + f_2 \frac{d\lambda_2}{d\tau} + f_3 \frac{d\lambda_3}{d\tau} \right) d\tau, \tag{9d}$$

$$\psi_p^h = \int_0^t \tau_c \left( \frac{d\gamma_{tp}}{d\tau} + \frac{d\gamma_{rp}}{d\tau} \right) d\tau, \tag{9e}$$

where  $\mathbf{C}$  is the fourth-ordered elasticity tensor.  $T_0$  is the balance temperature, and  $c$  is the heat capacity within a specific volume.  $F_1(T)$  and  $F_2(T)$  are two functions of temperature.  $f_1$ ,  $f_2$ , and  $f_3$  are the resistances of the transitions from the austenite to twinned martensite, the austenite to detwinned martensite and the twinned martensite to detwinned martensite phases, respectively, and are used to describe the hardening features of the martensite transformation and reorientation.  $\tau_c$  is the resistance to dislocation slipping.

Without considering the internal heat production caused by the dissipation of inelastic deformation, the well-known Clausius' dissipative inequality can be written as

$$\Gamma = \boldsymbol{\sigma} : \dot{\boldsymbol{\epsilon}} - \dot{\psi} - \eta \dot{T} \geq 0. \tag{10}$$

Substituting Eqs. (4), (8), and (9) into Eq. (10) yields

$$\Gamma = \underbrace{\left( \boldsymbol{\sigma} - \frac{\partial \psi^e}{\partial \boldsymbol{\epsilon}^e} \right) : \dot{\boldsymbol{\epsilon}}^e}_{\text{elasticity}} + \underbrace{\left( -\eta - \frac{\partial \psi^T}{\partial T} \right) \dot{T}}_{\text{entropy}}$$

$$\begin{aligned}
 & + (\boldsymbol{\sigma} + \mathbf{B}_{tr}) : \dot{\boldsymbol{\epsilon}}^{tr} + (\boldsymbol{\sigma} + \mathbf{B}_{reo}) : \dot{\boldsymbol{\epsilon}}^{reo} - \underbrace{\frac{\partial \psi^T}{\partial \lambda_1} \dot{\lambda}_1 - \frac{\partial \psi^T}{\partial \lambda_2} \dot{\lambda}_2 - \sum_{\alpha=1}^3 f_\alpha \dot{\lambda}_\alpha}_{\text{transformation and reorientation dissipation}} \\
 & + \underbrace{\boldsymbol{\sigma} : \dot{\boldsymbol{\epsilon}}^{tp} + \boldsymbol{\sigma} : \dot{\boldsymbol{\epsilon}}^{rp} - \tau_c (\dot{\gamma}_{tp} + \dot{\gamma}_{rp})}_{\text{plasticity dissipation}} \geq 0, \tag{11}
 \end{aligned}$$

Equation (11) is the total dissipation which consists of the elastic, entropy, and plastic parts as well as the ones related to the martensite transformation and reorientation. Since the elastic and entropy parts of the dissipation are always zero, this yields

$$\boldsymbol{\sigma} = \frac{\partial \psi^e}{\partial \boldsymbol{\epsilon}^e} = \mathbf{C} : \boldsymbol{\epsilon}^e, \tag{12a}$$

$$\eta = -\frac{\partial \psi^T}{\partial T} = c \ln \left( \frac{T}{T_0} \right) + \frac{dF_1}{dT} \lambda_1 + \frac{dF_2}{dT} \lambda_2, \tag{12b}$$

Considering Eqs. (5), (6), (7), and (12), Eq. (11) can be rewritten as

$$\begin{aligned}
 \Gamma = & - \left( \frac{\partial \psi^T}{\partial \lambda_1} + f_1 \right) \dot{\lambda}_1 + \left[ g (\boldsymbol{\sigma} + \mathbf{B}_{tr}) : \mathbf{N}_{tr} - \frac{\partial \psi^T}{\partial \lambda_2} - f_2 \right] \dot{\lambda}_2 \\
 & + [g (\boldsymbol{\sigma} + \mathbf{B}_{reo}) : \mathbf{N}_{reo} - f_3] \dot{\lambda}_3 \\
 & + (\boldsymbol{\sigma} : \mathbf{N}_{tr} - \tau_c) \dot{\gamma}_{tp} + (\boldsymbol{\sigma} : \mathbf{N}_{reo} - \tau_c) \dot{\gamma}_{rp} \geq 0. \tag{13}
 \end{aligned}$$

Stricter constraints for the dissipation inequality are introduced here as

$$\Gamma_{A \rightarrow M_t} = \pi_{A \rightarrow M_t} \dot{\lambda}_1 \geq 0, \tag{14a}$$

$$\Gamma_{A \rightarrow M_d} = \pi_{A \rightarrow M_d} \dot{\lambda}_2 \geq 0, \tag{14b}$$

$$\Gamma_{M_t \rightarrow M_d} = \pi_{M_t \rightarrow M_d} \dot{\lambda}_3 \geq 0, \tag{14c}$$

$$\Gamma_{tp} = \pi_{tp} \dot{\gamma}_{tp} \geq 0, \tag{14d}$$

$$\Gamma_{rp} = \pi_{rp} \dot{\gamma}_{rp} \geq 0, \tag{14e}$$

where  $\Gamma_{A \rightarrow M_t}$ ,  $\Gamma_{A \rightarrow M_d}$ ,  $\Gamma_{M_t \rightarrow M_d}$ ,  $\Gamma_{tp}$ , and  $\Gamma_{rp}$  are the dissipation parts for the transitions from the austenite to twinned martensite, the austenite to detwinned martensite, the twinned martensite to detwinned martensite, the transformation-induced and reorientation-induced plasticity, respectively.  $\pi_{A \rightarrow M_t}$ ,  $\pi_{A \rightarrow M_d}$ ,  $\pi_{M_t \rightarrow M_d}$ ,  $\pi_{tp}$ , and  $\pi_{rp}$  are the corresponding thermodynamic driving forces, and are defined as

$$\pi_{A \rightarrow M_t} = -[F_1(T) + f_1], \tag{15a}$$

$$\pi_{A \rightarrow M_d} = g (\boldsymbol{\sigma} + \mathbf{B}_{tr}) : \mathbf{N}_{tr} - F_2(T) - f_2, \tag{15b}$$

$$\pi_{M_t \rightarrow M_d} = g (\boldsymbol{\sigma} + \mathbf{B}_{reo}) : \mathbf{N}_{reo} - f_3, \tag{15c}$$

$$\pi_{tp} = \boldsymbol{\sigma} : \mathbf{N}_{tr} - \tau_c, \tag{15d}$$

$$\pi_{rp} = \boldsymbol{\sigma} : \mathbf{N}_{reo} - \tau_c, \tag{15e}$$

where  $F_1(T) = \frac{\partial \psi^T}{\partial \lambda_1}$  and  $F_2(T) = \frac{\partial \psi^T}{\partial \lambda_2}$ . Equation (14) describes the thermodynamic constraints on the constitutive

model, which means that the evolutions of  $\dot{\lambda}_1$ ,  $\dot{\lambda}_2$ ,  $\dot{\lambda}_3$ ,  $\dot{\gamma}_{tp}$ , and  $\dot{\gamma}_{rp}$  are not arbitrary.

## 2.4 Evolution equations for internal variables

### 2.4.1 Internal variables related to martensite transformation, reorientation, and plasticity

We adopt a rate-independent framework for describing the martensite transformation and reorientation, since the rate-dependent mechanical behavior of NiTi SMA is mainly caused by the SMA's strong thermo-mechanically coupled nature rather than its viscosity [29–31], i.e., for  $\dot{\lambda}_1$

$$\dot{\lambda}_1 = 0, \quad \text{no constraint}, \tag{16a}$$

$$\dot{\lambda}_1 > 0, \quad \pi_{A \rightarrow M_t} = Y_{A \rightarrow M_t}, \tag{16b}$$

$$\dot{\lambda}_1 < 0, \quad \pi_{A \rightarrow M_t} = -Y_{A \rightarrow M_t}, \tag{16c}$$

for  $\dot{\lambda}_2$

$$\dot{\lambda}_2 = 0, \quad \text{no constraint}, \tag{17a}$$

$$\dot{\lambda}_2 > 0, \quad \pi_{A \rightarrow M_d} = Y_{A \rightarrow M_d}, \tag{17b}$$

$$\dot{\lambda}_2 < 0, \quad \pi_{A \rightarrow M_d} = -Y_{A \rightarrow M_d}, \tag{17c}$$

for  $\dot{\lambda}_3$

$$\dot{\lambda}_3 = 0, \quad \text{no constraint}, \tag{18a}$$

$$\dot{\lambda}_3 > 0, \quad \pi_{M_t \rightarrow M_d} = Y_{M_t \rightarrow M_d}, \tag{18b}$$

where  $Y_{A \rightarrow M_t}$  is a variable controlling the temperature difference between  $M_f$  and  $A_s$  (the start temperature of the reverse transformation) during the transition between the austenite and twinned martensite phases.  $Y_{A \rightarrow M_d}$  is a variable controlling the width of the stress-strain hysteresis loop during the transition between the austenite and detwinned martensite phases.  $Y_{M_t \rightarrow M_d}$  is a material parameter controlling the initial start stress of martensite reorientation.

If the rates  $\dot{\lambda}_1$ ,  $\dot{\lambda}_2$ , and  $\dot{\lambda}_3$  are non-zero, the following consistent conditions should be satisfied.

For the transition from the austenite to twinned martensite

$$\dot{\lambda}_1 (\dot{\pi}_{A \rightarrow M_t} - \dot{Y}_{A \rightarrow M_t}) = 0, \quad \text{if } \pi_{A \rightarrow M_t} - Y_{A \rightarrow M_t} = 0; \tag{19a}$$

from the twinned martensite to austenite

$$\dot{\lambda}_1 (\dot{\pi}_{A \rightarrow M_t} + \dot{Y}_{A \rightarrow M_t}) = 0, \quad \text{if } \pi_{A \rightarrow M_t} + Y_{A \rightarrow M_t} = 0; \tag{19b}$$

from the austenite to detwinned martensite

$$\dot{\lambda}_2 (\dot{\pi}_{A \rightarrow M_d} - \dot{Y}_{A \rightarrow M_d}) = 0, \quad \text{if } \pi_{A \rightarrow M_d} - Y_{A \rightarrow M_d} = 0; \tag{19c}$$

from the detwinned martensite to austenite

$$\dot{\lambda}_2 (\dot{\pi}_{A \rightarrow M_d} + \dot{Y}_{A \rightarrow M_d}) = 0, \quad \text{if } \pi_{A \rightarrow M_d} + Y_{A \rightarrow M_d} = 0; \tag{19d}$$

from the twinned martensite to detwinned martensite

$$\dot{\lambda}_3 (\dot{\pi}_{M_t \rightarrow M_d} - \dot{Y}_{M_t \rightarrow M_d}) = 0, \quad \text{if } \pi_{M_t \rightarrow M_d} - Y_{M_t \rightarrow M_d} = 0. \tag{19e}$$

Equation (19) is used to determine the rates  $\dot{\lambda}_1$ ,  $\dot{\lambda}_2$ , and  $\dot{\lambda}_3$ . The two temperature functions  $F_1(T)$  and  $F_2(T)$  are chosen as

$$F_1(T) = \beta(T - M_s) - Y_{A \rightarrow M_t}, \tag{20a}$$

$$F_2(T) = \begin{cases} \beta(T - M_s) - Y_{A \rightarrow M_d}, & \dot{\lambda}_2 \geq 0, \\ \beta(T - M_s) - Y_{A \rightarrow M_d}, & \dot{\lambda}_2 < 0, \end{cases} \tag{20b}$$

where  $\beta$  is a constant, called the coefficient of entropy difference between the austenite and martensite phases, and is used to describe the dependence of the martensite transformation on the temperature.  $\langle x \rangle$  is the McCauley bracket: when  $x \geq 0$ ,  $\langle x \rangle = x$ ; when  $x < 0$ ,  $\langle x \rangle = 0$ . The McCauley bracket in Eq. (20b) is used to ensure the transition from the austenite to the detwinned martensite phase cannot occur during cooling in a stress-free and dislocation-free case.

Considering the effect of the martensite transformation on the dislocation slippage, the evolution equation of the transformation-induced plasticity is proposed as

$$\dot{\gamma}_{tp} = \xi_A \gamma_0 \left( \frac{\boldsymbol{\sigma} : \mathbf{N}_{tr}}{\mu} \right)^2 \exp \left\{ \frac{-\Delta G_{slip}}{k_b T} \left[ 1 - \left( \frac{\pi_{tp}}{\tau_0} \right)^p \right]^q \right\} \times (|\dot{\lambda}_1| + |\dot{\lambda}_2|), \quad \text{if } \pi_{tp} > 0, \tag{21a}$$

$$\dot{\gamma}_{tp} = 0, \quad \text{if } \pi_{tp} \leq 0, \tag{21b}$$

where  $\gamma_0$  is the reference slipping rate,  $p$  and  $q$  are material parameters with the constraints of  $0 < p \leq 1$  and  $1 < q \leq 2$ ,  $\mu$  is the shear modulus,  $\Delta G_{slip}$  is the activation energy of dislocation slipping in a stress-free configuration,  $k_b$  is Boltzmann's constant, and  $\tau_0$  is the resolved shear stress required to overcome the Peierl's obstacles at  $T = 0$  K. The term  $|\dot{\lambda}_1| + |\dot{\lambda}_2|$  reflects that the plastic deformation is induced by the martensite transformation. The term  $\xi_A$  reflects that the dislocation slipping related to the transformation-induced plasticity occurs only in the austenite phase.

Similarly, the evolution equation of the reorientation-induced plasticity is proposed as

$$\dot{\gamma}_{rp} = (1 - \xi_A) \gamma_0 \left( \frac{\boldsymbol{\sigma} : \mathbf{N}_{reo}}{\mu} \right)^2 \exp \left\{ \frac{-\Delta G_{slip}}{k_b T} \left[ 1 - \left( \frac{\pi_{rp}}{\tau_0} \right)^p \right]^q \right\} \times |\dot{\lambda}_3|, \quad \text{if } \pi_{rp} > 0, \tag{22a}$$

$$\dot{\gamma}_{rp} = 0, \quad \text{if } \pi_{rp} \leq 0. \tag{22b}$$

The term  $|\dot{\lambda}_3|$  reflects that the plastic deformation is induced by the martensite reorientation. The term  $(1 - \xi_A)$  reflects that the dislocation slippage related to the reorientation-induced plasticity occurs only in the martensite phase.

The evolution equation of dislocation density can be described by the equation proposed by Mecking and Kocks [32]:

$$\dot{\rho}^\alpha = (k_1 \sqrt{\rho} - k_2 \rho) (\dot{\gamma}_{tp} + \dot{\gamma}_{rp}), \tag{23}$$

where  $\rho$  is the dislocation density at a material point,  $k_1$  and  $k_2$  are two material parameters. The terms  $k_1 \sqrt{\rho}$  and  $k_2 \rho$  represent the dislocation multiplication and annihilation, respectively.

The slipping resistance  $\tau_c$  progressively increases during the cyclic deformation, which is caused by the increasing density of forest dislocation and can be written as [32]

$$\tau_c = \frac{1}{2} \mu b \sqrt{\rho}, \tag{24}$$

where  $b$  is the magnitude of Burgers vector for the NiTi SMA.

#### 2.4.2 Internal variables related to the degeneration of shape memory effect

Recently, to address the effect of dislocation slipping on the martensite transformation, Yu et al. [19,20] proposed some specific evolution laws to link the internal variables controlling the degeneration of super-elasticity and the current dislocation density. In this work, such an approach is extended to address the effect of dislocation slipping on both the martensite transformation and reorientation.

It is assumed that the orientations of  $\mathbf{B}_{tr}$  and  $\mathbf{B}_{reo}$  coincide with the orientations of martensite transformation and reorientation, i.e.,

$$\mathbf{B}_{tr} = B_{tr}^n \frac{\mathbf{N}_{tr}}{\|\mathbf{N}_{tr}\|}, \tag{25a}$$

$$\mathbf{B}_{reo} = B_{reo}^n \frac{\mathbf{N}_{reo}}{\|\mathbf{N}_{reo}\|}, \tag{25b}$$

where  $B_{tr}^n$  and  $B_{reo}^n$  are the norms of  $\mathbf{B}_{tr}$  and  $\mathbf{B}_{reo}$ , respectively. From Eq. (25), it is seen that the two tensors  $\mathbf{B}_{tr}$  and  $\mathbf{B}_{reo}$  can be obtained once the two scalars  $B_{tr}^n$  and  $B_{reo}^n$  are known.

The evolutions of  $B_{tr}^n$  and  $B_{reo}^n$  are assumed to be governed by the following equations:

$$\dot{B}_{tr}^n = d(c_1\sqrt{\rho} - B_{tr}^n) \left( \sum_{i=1}^3 |\dot{\lambda}_i| \right), \quad (26a)$$

$$\dot{B}_{reo}^n = d(c_2\sqrt{\rho} - B_{reo}^n) \left( \sum_{i=1}^3 |\dot{\lambda}_i| \right), \quad (26b)$$

where  $d$ ,  $c_1$ , and  $c_2$  are material parameters.

Based on experimental observations [7], three hardening functions,  $f_1$ ,  $f_2$ , and  $f_3$  are proposed as

$$f_1 = H_{A \rightarrow M_t} \xi_M^t, \quad (27a)$$

$$f_2 = H_{A \rightarrow M_d} \xi_M^d, \quad (27b)$$

$$f_3 = H_{M_t \rightarrow M_d}^I (\xi_M^d - \tilde{\lambda}_2) + H_{M_t \rightarrow M_d}^{II} (\xi_M^d - \lambda_{ref}), \quad (27c)$$

where  $H_{A \rightarrow M_t}$  and  $H_{A \rightarrow M_d}$  are the hardening moduli for the transitions between the austenite and twinned martensite phases, and the austenite and detwinned martensite phases, respectively. From experimental observations, it is seen that the hardening caused by the martensite reorientation can be divided into two stages: stage I and stage II. At each stage, the reorientation hardening exhibits approximate linearity, and the hardening modulus at stage II is much larger than that at stage I.  $H_{M_t \rightarrow M_d}^I$  and  $H_{M_t \rightarrow M_d}^{II}$  are the hardening moduli for the martensite reorientation.  $\lambda_{ref}$  is a material parameter. It should be noted that since the increment of the reorientation modulus at stage II is not very large [7], the evolutions of  $H_{M_t \rightarrow M_d}^{II}$  are not considered for simplicity here.  $\tilde{\lambda}_2$  is a variable defined as

$$\dot{\tilde{\lambda}}_2 = \dot{\lambda}_2, \quad \text{if } (\dot{\lambda}_2 > 0) \text{ or } (\dot{\lambda}_2 < 0 \text{ and } \tilde{\lambda}_2 > 0). \quad (28)$$

It should be noted that the variable  $\tilde{\lambda}_2$  is introduced here to ensure that the first term in the right side of Eq. (27c) can be recovered to zero after each loading–unloading–heating–cooling cycle, and does not influence the start stress of martensite reorientation (the evolution of the start stress of martensite reorientation is controlled only by the variable  $B_{reo}$ ).

The martensite transformation and reorientation moduli, i.e.,  $H_{A \rightarrow M_d}$  and  $H_{M_t \rightarrow M_d}^I$  can be decomposed as

$$H_{A \rightarrow M_d} = H_{A \rightarrow M_d}^f + H_{A \rightarrow M_d}^\rho, \quad (29a)$$

$$H_{M_t \rightarrow M_d}^I = H_{M_t \rightarrow M_d}^{If} + H_{M_t \rightarrow M_d}^{I\rho}, \quad (29b)$$

where  $H_{A \rightarrow M_d}^f$  and  $H_{M_t \rightarrow M_d}^{If}$  are two constants that are used to reflect the transformation and reorientation hardening features of NiTi SMA in a dislocation-free state, respectively.

$H_{A \rightarrow M_d}^\rho$  and  $H_{M_t \rightarrow M_d}^{I\rho}$  are, respectively, the additional transformation and reorientation hardening moduli caused by the increasing dislocation density.

The evolution equations of  $H_{A \rightarrow M_d}^\rho$  and  $H_{M_t \rightarrow M_d}^{I\rho}$  are given as

$$\dot{H}_{A \rightarrow M_d}^\rho = d(c_3\sqrt{\rho} - H_{A \rightarrow M_d}^\rho) \left( \sum_{i=1}^3 |\dot{\lambda}_i| \right), \quad (30a)$$

$$\dot{H}_{M_t \rightarrow M_d}^{I\rho} = d(c_4\sqrt{\rho} - H_{M_t \rightarrow M_d}^{I\rho}) \left( \sum_{i=1}^3 |\dot{\lambda}_i| \right), \quad (30b)$$

where  $c_3$  and  $c_4$  are two material parameters.

The variable  $Y_{A \rightarrow M_d}$  controls the width of the stress-strain hysteresis loop. Similarly, it can be decomposed as

$$Y_{A \rightarrow M_d} = Y_{A \rightarrow M_d}^f - Y_{A \rightarrow M_d}^\rho, \quad (31)$$

where  $Y_{A \rightarrow M_d}^f$  is the value of  $Y_{A \rightarrow M_d}$  under the dislocation-free condition and is a constant, while  $Y_{A \rightarrow M_d}^\rho$  represents the effect of dislocation slipping on the stress-strain hysteresis loop and is a function of the current dislocation density. The evolution equation of  $Y_{A \rightarrow M_d}^\rho$  is given as:

$$\dot{Y}_{A \rightarrow M_d}^\rho = d(c_5\sqrt{\rho} - Y_{A \rightarrow M_d}^\rho) \left( \sum_{i=1}^3 |\dot{\lambda}_i| \right), \quad (32)$$

where  $c_5$  is a material parameter.

### 3 Determination of parameters

In the experimental observations of Kan et al. [7], the experimental material was a NiTi SMA sheet (Ni 50.9% at mass, from Jiangyin Materials Development Co. Ltd., China). The finish temperature of martensite  $M_f$ , the start temperature of martensite  $M_s$ , the finish temperature of austenite  $A_f$  and the start temperature of austenite  $A_s$  were 308, 323, 375, and 357 K, respectively. The test temperature (i.e., 299 K) was lower than  $M_f$ , and the initial phase of the sheet was the twinned martensite phase. In each thermo-mechanical cycle, the specimen was first loaded to the peak stress, and then unloaded to zero stress. After the mechanical loading and unloading, the specimen was heated to 393 K and finally cooled to the test temperature.

The material parameters used in the proposed model will be determined from the cyclic stress–strain–temperature curves with the peak stress of 850 MPa in Ref. [7]. The solid and dashed lines in Fig. 3a show the experimental cyclic stress-strain curves in the first and tenth cycles, respectively, with the peak stress of 850 MPa [7]. The solid and dashed



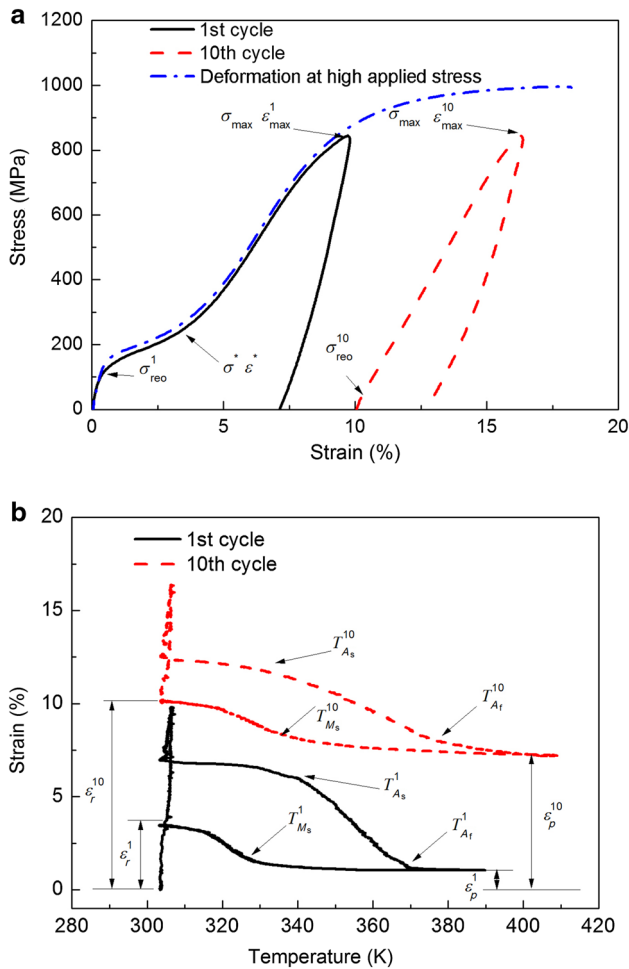


**Fig. 3** Stress-strain-temperature curves used to determine the material parameters for the proposed model. **a** Stress-strain curves. **b** Strain-temperature curves

lines in Fig. 3b show the corresponding cyclic temperature-strain curves in the first and tenth cycles, respectively. It is seen that the start stresses of martensite reorientation in the first and tenth cycles are denoted as  $\sigma_{\text{re}}^1$  and  $\sigma_{\text{re}}^{10}$ , respectively. The maximum stresses/strains in the first and tenth cycles are denoted as  $\sigma_{\text{max}}^1$ ,  $\varepsilon_{\text{max}}^1$ , and  $\sigma_{\text{max}}^{10}$ ,  $\varepsilon_{\text{max}}^{10}$ , respectively. The stress and strain at the inflection point in the first cycle are denoted as  $\sigma^*$  and  $\varepsilon^*$ , respectively. The start temperatures of the forward transformation and its reverse, and the finish temperature of reverse transformation in the first cycle are denoted as  $T_{Ms}^1$ ,  $T_{As}^1$ , and  $T_{Af}^1$ , respectively, and they are denoted as  $T_{Ms}^{10}$ ,  $T_{As}^{10}$ , and  $T_{Af}^{10}$  in the tenth cycle. The plastic strains in the first and tenth cycles are denoted as  $\varepsilon_p^1$  and  $\varepsilon_p^{10}$ , respectively, and the residual strains in the first and tenth cycles are denoted as  $\varepsilon_r^1$  and  $\varepsilon_r^{10}$ , respectively.

### 3.1 Physical constants

Since the cyclic deformation of polycrystalline NiTi SMA is discussed here, the elasticity tensor  $C$  is assumed to be isotropic, i.e.,

$$C = \frac{E\nu}{(1-2\nu)(1+\nu)}\delta \otimes \delta + \frac{E}{(1+\nu)}I, \quad (33a)$$

$$I_{ijkl} = \frac{1}{2}(\delta_{il}\delta_{jk} + \delta_{ik}\delta_{jl}), \quad (33b)$$

where  $E$  and  $\nu$  are the elastic modulus and Poisson's ratio, respectively.  $\delta$  and  $I$  are the second-order unit tensor and fourth-order identity tensor, respectively.  $\nu$  is set as 0.33 by referring to Ref. [15]. The elasticity parameters of the austenite and martensite phases are assumed to be identical here, and can be obtained directly from Fig. 3a, i.e.,  $E = 35$  GPa. Referring to the existing literature [32,33], the physical constants  $\Delta G_{\text{slip}}$ ,  $k_b$ , and  $b$  are set to be  $2.5 \times 10^{-19} \text{ J}^{-1}$ ,  $1.38 \times 10^{-23} \text{ J/K}$  and  $3.6 \times 10^{-10} \text{ m}$ , respectively. The parameters  $k_1$  and  $k_2$  which control the evolution of dislocation density are set to be  $1.5 \times 10^{10} \text{ m}$  and 100, respectively.

### 3.2 Parameters related to martensite transformation, reorientation, and plasticity

The four parameters  $p$ ,  $q$ ,  $\gamma_0$ ,  $\tau_0$ , and  $d$  control the saturated value and rate of the plastic strain. However, they cannot be determined directly since Eqs. (21a) and (22a) cannot be integrated. Thus, they can only be obtained by the trial-and-error method from the evolution curve of plastic strain with a peak stress of 850 MPa.

The parameter  $g$  controls the maximum reorientation/transformation strain, and is set as 0.1. The parameters,  $H_{A \rightarrow M_t}$ ,  $Y_{A \rightarrow M_t}$ ,  $H_{A \rightarrow M_d}^f$ ,  $Y_{A \rightarrow M_d}^f$ ,  $\lambda_{\text{ref}}$ ,  $Y_{M_t \rightarrow M_d}$ ,  $H_{M_t \rightarrow M_d}^f$ ,  $c_1$ ,  $c_2$ ,  $c_3$ , and  $c_5$  can be determined directly from the critical points defined in the cyclic temperature-stress-strain curves. In this section, only the final forms of the above mentioned parameters are given; the detailed derivation can be found in the Appendix.

$$Y_{M_t \rightarrow M_d} = g\sigma_{\text{re}}^1, \quad (34a)$$

$$\lambda_{\text{ref}} = \frac{\varepsilon^* - \frac{\sigma^*}{E}}{g}, \quad (34b)$$

$$H_{M_t \rightarrow M_d}^f = \frac{g\sigma^* - Y_{M_t \rightarrow M_d}}{\lambda_{\text{ref}}}, \quad (34c)$$

$$H_{A \rightarrow M_t} = \beta(M_s - M_f), \quad (34d)$$

$$Y_{A \rightarrow M_t} = \frac{\beta(A_s - M_f)}{2}, \quad (34e)$$

**Table 1** Material parameters used in the proposed model

Elastic constants:

$$E = 35 \text{ GPa}; \nu = 0.33$$

Physical constants:

$$\Delta G_{\text{slip}} = 2.5 \times 10^{-19} \text{ J}^{-1}; k_b = 1.38 \times 10^{-23} \text{ J/K}; b = 3.6 \times 10^{-10} \text{ m}$$

Parameters related to martensite transformation:

$$g = 0.1; \beta = 0.5 \text{ MPa/K}; H_{A \rightarrow M_t} = 12.5 \text{ MPa}; Y_{A \rightarrow M_t} = 12.25 \text{ MPa}; H_{A \rightarrow M_d}^f = 24.77 \text{ MPa};$$

$$Y_{A \rightarrow M_d}^f = 8.85 \text{ MPa}; c_1 = 1.07 \text{ N/m}; c_3 = 0.16 \text{ N/m}; c_5 = 0.025 \text{ N/m}; d = 0.2$$

Parameters related to martensite reorientation:

$$Y_{M_t \rightarrow M_d} = 15 \text{ MPa}; H_{M_t \rightarrow M_d}^I = 32.4 \text{ MPa}; H_{M_t \rightarrow M_d}^{II} = 200 \text{ MPa}; \lambda_{\text{ref}} = 0.31; c_2 = 0.96 \text{ N/m}; c_4 = 0.7 \text{ N/m}$$

Parameters related to dislocation slipping:

$$k_1 = 1.5 \times 10^{10} \text{ m}; k_2 = 100; p = 0.05; q = 1, \gamma_0 = 2, \tau_0 = 200 \text{ MPa}$$

$$\begin{Bmatrix} H_{A \rightarrow M_d}^f \\ Y_{A \rightarrow M_d}^0 \\ c_1 \\ c_3 \\ c_5 \end{Bmatrix} = \begin{bmatrix} -\xi_d^{\text{max},1} & 2 & gR & -R\xi_d^{\text{max},1} & -2R \\ 0 & 2 & gP & 0 & -2P \\ -\xi_d^{\text{max},10} & 2 & g\sqrt{\rho_{10}} & -\sqrt{\rho_{10}}\xi_d^{\text{max},10} & -2\sqrt{\rho_{10}} \\ 0 & 2 & g\sqrt{\rho_{10}} & 0 & -2\sqrt{\rho_{10}} \\ -\xi_d^{Mf,10} & 0 & g\sqrt{\rho_{10}} & -\sqrt{\rho_{10}}\xi_d^{Mf,10} & 0 \end{bmatrix}^{-1} \times \begin{Bmatrix} \beta(T_{As}^1 - M_s) \\ \beta(T_{Af}^1 - M_s) \\ \beta(T_{As}^{10} - M_s) \\ \beta(T_{Af}^{10} - M_s) \\ \beta(T_{Mf}^{10} - M_s) \end{Bmatrix}, \tag{34f}$$

$$c_2 = \frac{Y_{M_t \rightarrow M_d} - \sigma_{\text{reo}}^{10}}{g\sqrt{\rho_{10}}}, \tag{34g}$$

where

$$\sqrt{\rho_1} = \frac{k_1}{k_2} \left( 1 - e^{-\frac{k_2 \varepsilon_p^1}{2}} \right), \tag{35a}$$

$$\sqrt{\rho_{10}} = \frac{k_1}{k_2} \left( 1 - e^{-\frac{k_2 \varepsilon_p^{10}}{2}} \right), \tag{35b}$$

$$\xi_d^{\text{max},1} = \frac{\varepsilon_{\text{max}}^1 - \frac{\sigma_{\text{max}}^1}{E} - \varepsilon_p^1}{g}, \tag{35c}$$

$$\xi_d^{\text{max},10} = \frac{\varepsilon_{\text{max}}^{10} - \frac{\sigma_{\text{max}}^{10}}{E} - \varepsilon_p^{10}}{g}, \tag{35d}$$

$$R = \sqrt{\rho_1} \left( 1 - e^{-d\xi_d^{\text{max},1}} \right), \tag{35e}$$

$$P = \sqrt{\rho_1} \left( 1 - e^{-2d\xi_d^{\text{max},1}} \right). \tag{35f}$$

The parameter  $c_4$  is set as 0.7 N/m by fitting the increment of reorientation hardening modulus at stage I.  $H_{M_t \rightarrow M_d}^{II}$  is set as 200 MPa by fitting the reorientation hardening modulus at stage II.

All the material parameters are listed in Table 1.

### 4 Verification and discussion

By using the material parameters listed in Table 1, the proposed model is used to describe the cyclic degeneration of shape memory effect occurring in the thermo-mechanical cyclic deformation of NiTi SMA. Since the initial phase of the specimen is the twinned martensite phase, the initial volume fractions of three prescribed phases, i.e.,  $\xi_A^0$ ,  $\xi_M^0$ , and  $\xi_M^{d0}$  are set as 0, 1, and 0, respectively. The simulated cyclic stress-strain and strain-temperature curves obtained in the stress-controlled thermo-mechanical cyclic test with the peak stresses of 500, 750, and 850 MPa are shown in Figs. 4–6.

From the figures, it is seen that: (1) The simulated results are in good agreement with the experimental ones for the case with a peak stress of 850 MPa. Two stages of martensite reorientation hardening, decreased start stress of martensite reorientation, increased temperature of martensite transformation, increased transformation and reorientation hardening moduli, and new inelastic deformation occurring in the cooling process in each cycle, are well captured by the proposed model. However, this good agreement is expected because the material parameters used in the proposed model are calibrated from the experimental data obtained in this case. (2) Although the parameters are determined only by the stress-strain-temperature curves with the peak stress of 850 MPa, the cyclic degeneration of shape memory effect occurring in the cyclic tests of NiTi SMAs with two other peak stresses (500 and 750 MPa) can be well predicted, too.

Figure 7 shows the evolution curves of residual, plastic and peak strains, respectively. Comparing with the experimental results, we conclude that the dependence of the cyclic degeneration of shape memory effect on the applied loading level can be described reasonably by the proposed model, since the corresponding physical mechanism is considered here.

The evolution curves of three phases ( $A$ ,  $M^t$ , and  $M^d$ ) in the mechanical loading–unloading and heating–cooling pro-

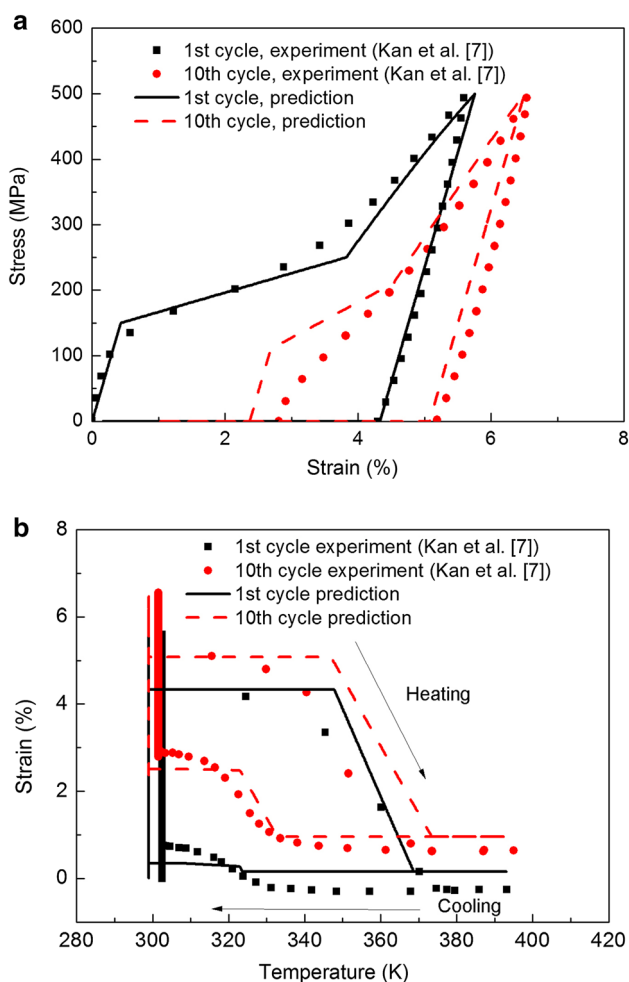


**Fig. 4** Degeneration of shape memory effect in the cyclic test of NiTi SMA with a peak stress of 500 MPa. **a** Stress-strain curves in the 1st and 10th cycles. **b** Temperature-strain curves in the 1st and 10th cycles

cesses in the first cycle are given in Fig. 8a and b, respectively. From Fig. 8a, it is seen that at the beginning of the first cycle, the material consists of the twinned martensite phase and no macroscopic strain can be observed. When the applied stress reaches a critical value, martensite reorientation (i.e., the transition from the twinned martensite to the detwinned one) occurs, the volume fraction of twinned martensite (from point  $a' \rightarrow$  point  $b'$  in Fig. 8a) decreases, while that of detwinned martensite (from point  $a \rightarrow$  point  $b$  in Fig. 8a) increases. In the mechanical unloading process, we see that the volume fractions of the twinned and detwinned martensite phases stay constant (from point  $b' \rightarrow$  point  $c'$  and point  $b \rightarrow$  point  $c$  in Fig. 8a), since only elastic deformation occurs. In the heating process, the reverse transformation (i.e., the transition from the twinned martensite to austenite and from the detwinned martensite to austenite) occurs when the temperature reaches a critical value. Thus, it is seen that the volume fractions of the twinned ( $d' \rightarrow e' \rightarrow f' \rightarrow g'$  in Fig. 8b)

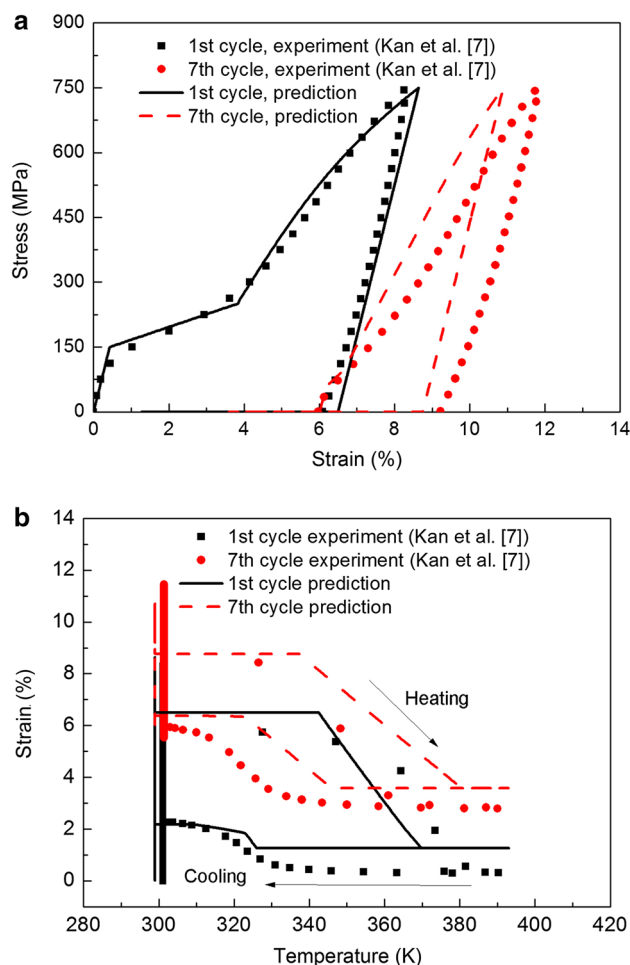


**Fig. 5** Degeneration of shape memory effect in the cyclic test of NiTi SMA with a peak stress of 750 MPa. **a** Stress-strain curves in the 1st and 7th cycles. **b** Temperature-strain curves in the 1st and 7th cycles

and detwinned martensite ( $d \rightarrow e \rightarrow f$  in Fig. 8b) decrease, simultaneously, while the volume fraction of the austenite increases ( $a'' \rightarrow b'' \rightarrow c''$ ). In the subsequent cooling process, from Eqs. (15a), (15b), (16b), (17b), (20a), and (20b), the transformation conditions from the twinned martensite to austenite and from the detwinned martensite to austenite can be written as (note that the applied stress is equal to zero)

$$-\beta (T - M_s) = 0, \tag{36a}$$

$$g \mathbf{B}_{tr} : \mathbf{N}_{tr} - \beta \langle T - M_s \rangle = 0. \tag{36b}$$

From Eq. (36a), we see that the transition from the twinned martensite phase to austenite occurs when  $T = M_s$  (i.e., point  $h'$  in Fig. 8b). From Eq. (36b), it can be concluded that the transition from the detwinned martensite to austenite cannot occur if the internal stress tensor  $\mathbf{B}_{tr}$  is a zero-tensor. However, the plastic deformation will be induced by the martensite reorientation in the mechanical loading–unloading process. In this condition, a self-balanced local



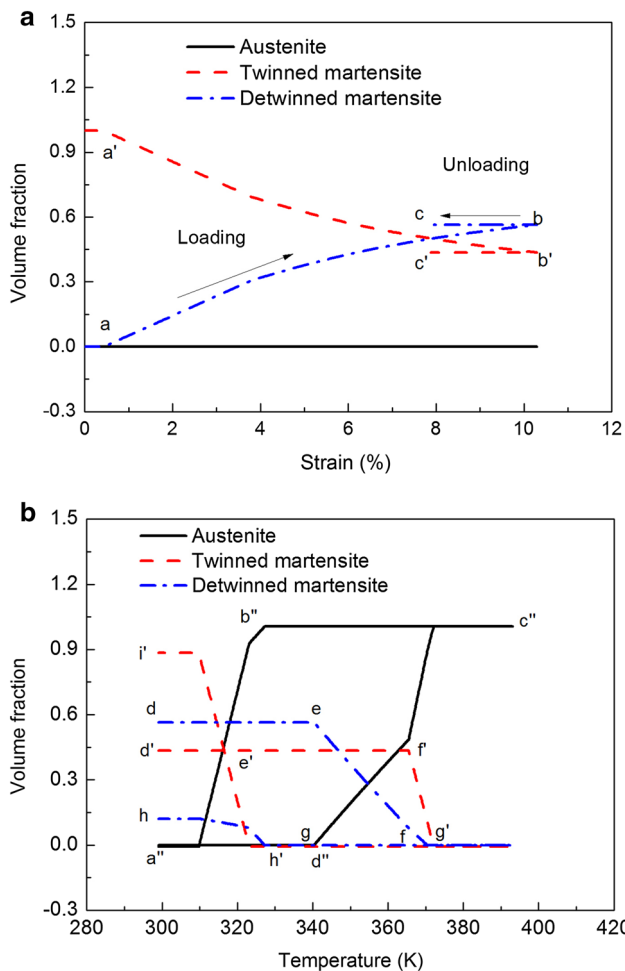


**Fig. 8** Evolution curves of three phases ( $A$ ,  $M^t$ , and  $M^d$ ) in the cyclic test of NiTi SMA with a peak stress of 850 MPa. **a** In mechanical loading–unloading process. **b** In heating–cooling process

### 5 Conclusions

- (1) Based on experimental observations [7], a macroscopic phenomenological constitutive model of NiTi SMAs is constructed in the framework of irreversible thermodynamics by addressing two inelastic deformation mechanisms, i.e., martensite transformation-induced and reorientation-induced plasticity. Three phases ( $A$ ,  $M^t$ , and  $M^d$ ) and the transformations between each pair of them are considered.
- (2) The evolution equations of internal variables are proposed by attributing the cyclic degeneration of shape memory effect to the interaction between the three phases ( $A$ ,  $M^t$ , and  $M^d$ ) and plastic deformation.
- (3) The new inelastic deformation occurring in the cooling process of each thermo-mechanical loading cycle comes from the transition from the twinned martensite phase to the detwinned one, and can be well predicted by the

proposed model once the internal stress tensor  $\mathbf{B}_{tr}$  is introduced.

- (4) Once various inelastic deformation mechanisms and their interactions are considered, the stress-strain-temperature curves and the loading level-dependent degeneration of shape memory effect can be well simulated and predicted by the proposed model.

**Acknowledgements** Financial supports by the National Natural Science Foundation of China (Grant 11532010) and the project for Sichuan Provincial Youth Science and Technology Innovation Team, China (Grant 2013TD0004) are appreciated.

### Appendix

Integrating Eq. (23) yields:

$$\sqrt{\rho} = \frac{k_1}{k_2} \left[ 1 - e^{-\frac{k_2}{2}(\gamma_{tp} + \gamma_{rp})} \right]. \tag{A1}$$

Equation (A1) is the explicit relationship between the slipage amount  $\gamma_{tp} + \gamma_{rp}$  and the dislocation density  $\rho$ . Thus, the dislocation densities after the first and tenth cycles can be obtained as

$$\sqrt{\rho_1} = \frac{k_1}{k_2} \left( 1 - e^{-\frac{k_2 \varepsilon_p^1}{2}} \right), \tag{A2a}$$

$$\sqrt{\rho_{10}} = \frac{k_1}{k_2} \left( 1 - e^{-\frac{k_2 \varepsilon_p^{10}}{2}} \right), \tag{A2b}$$

where  $\rho_1$  and  $\rho_{10}$  are the dislocation densities after the first and tenth cycles, respectively.

In the first loading cycle, the reorientation condition (Eq. 18b) at point  $\sigma_{reo}^1$  can be written as (note that  $\mathbf{B}_{reo}$  and  $f_3$  are both zero)

$$g\sigma_{reo}^1 = Y_{M_t \rightarrow M_d}. \tag{A3}$$

The parameter  $Y_{M_t \rightarrow M_d}$  can be determined by Eq. (A3), as shown in Eq. (34a).

At the inflection point ( $\sigma^*$ ,  $\varepsilon^*$ ), since the applied stress is very low, the plastic deformation can be neglected. In this condition, the total strain consists of the elastic strain and the transformation strain, i.e.,

$$\varepsilon^* = \frac{\sigma^*}{E} + g\lambda_{ref}. \tag{A4}$$

The parameter  $\lambda_{ref}$  can be obtained by Eq. (A4), as shown in Eq. (34b).

The reorientation condition at the inflection point can be written as

$$g\sigma^* - H_{M_t \rightarrow M_d}^I \lambda_{\text{ref}} = Y_{M_t \rightarrow M_d}. \quad (\text{A5})$$

The parameter  $H_{M_t \rightarrow M_d}^I$  can be obtained by Eq. (A5), as shown in Eq. (34c).

Considering the transition between the austenite and twinned martensite phases under the stress-free conditions, the transformation condition at the finish point of the forward transformation and the start point of the reverse transformation can be written as (by Eqs. (15a), (16b), (16c), and (20a))

$$-\left[\beta(M_f - M_s) - Y_{A \rightarrow M_t} + H_{A \rightarrow M_t}\right] = Y_{A \rightarrow M_t}, \quad (\text{A6a})$$

$$-\left[\beta(A_s - M_s) - Y_{A \rightarrow M_t} + H_{A \rightarrow M_t}\right] = -Y_{A \rightarrow M_t}. \quad (\text{A6b})$$

Two parameters  $H_{A \rightarrow M_t}$  and  $Y_{A \rightarrow M_t}$  can be obtained by Eq. (A6a) and (A6b), as shown in Eq. (34d) and (34e).

Rewrite Eqs. (26a), (26b), (29), and (31) in the following form

$$\dot{Z}_i = d(c_i \sqrt{\rho} - Z_i) \left( \sum_{i=1}^3 |\dot{\lambda}_i| \right), \quad i = 1, 2, 3, 4, 5, \quad (\text{A7})$$

where  $Z_1, Z_2, Z_3, Z_4$ , and  $Z_5$  represent  $B_{\text{tr}}^n, B_{\text{reo}}^n, H_{A \rightarrow M_d}^\rho, H_{M_t \rightarrow M_d}^\rho$ , and  $Y_{A \rightarrow M_d}^\rho$ , respectively. Note that Eq. (A7) cannot be integrated unless the  $\sqrt{\rho}$  is regarded as a constant in the first cycle. Thus, for simplicity, it is assumed that  $\sqrt{\rho}$  can be replaced by  $\sqrt{\rho_1}$  in Eq. (A7). Then, integrating Eq. (A7) yields:

$$Z_i = c_i \sqrt{\rho_1} \left[ 1 - \exp \left( -d \sum_{i=1}^3 \bar{\lambda}_i \right) \right], \quad i = 1, 2, 3, 4, 5, \quad (\text{A8})$$

where  $\bar{\lambda}_i = |\dot{\lambda}_i|$ .

From Eqs. (21a) and (22a), it can be concluded that the amount of dislocation slippage in the loading part is much larger than that in the unloading and cooling/heating processes. Thus, in the first and tenth cycles, the plastic strains at maximum stress points are approximately equal to  $\varepsilon_p^1$  and  $\varepsilon_p^{10}$ , respectively. Thus, the maximum strains in the first and tenth cycles can be given as

$$\varepsilon_{\text{max}}^1 = \frac{\sigma_{\text{max}}^1}{E} + g\xi_{\text{d}}^{\text{max},1} + \varepsilon_p^1, \quad (\text{A9a})$$

$$\varepsilon_{\text{max}}^{10} = \frac{\sigma_{\text{max}}^{10}}{E} + g\xi_{\text{d}}^{\text{max},10} + \varepsilon_p^{10}. \quad (\text{A9b})$$

By Eq. (A9), the maximum volume fraction of the detwinned martensite in the first cycle, i.e.,  $\xi_{\text{d}}^{\text{max},1}$  can be obtained as

$$\xi_{\text{d}}^{\text{max},1} = \frac{\varepsilon_{\text{max}}^1 - \frac{\sigma_{\text{max}}^1}{E} - \varepsilon_p^1}{g}, \quad (\text{A10a})$$

$$\xi_{\text{d}}^{\text{max},10} = \frac{\varepsilon_{\text{max}}^{10} - \frac{\sigma_{\text{max}}^{10}}{E} - \varepsilon_p^{10}}{g}. \quad (\text{A10b})$$

By Eq. (A8), the variable  $Z_i$  at the start and finish points, respectively, of reverse transformation in the first cycle can be written as

$$Z_{i,As}^1 = c_i \sqrt{\rho_1} \left[ 1 - \exp \left( -d\xi_{\text{d}}^{\text{max},1} \right) \right], \quad i = 1, 2, 3, 4, 5, \quad (\text{A11a})$$

$$Z_{i,Af}^1 = c_i \sqrt{\rho_1} \left[ 1 - \exp \left( -2d\xi_{\text{d}}^{\text{max},1} \right) \right], \quad i = 1, 2, 3, 4, 5. \quad (\text{A11b})$$

For the transition between the austenite and detwinned martensite phases, the transformation conditions at the start and finish points of reverse transformation in the first cycle can be written as, respectively (by Eqs. (15b), (17b), (17c), (20b), (26)–(31))

$$g c_1 R - \beta \left( T_{As}^1 - M_s \right) + Y_{A \rightarrow M_d}^f - c_5 R - \left( H_{A \rightarrow M_d}^f + c_3 R \right) \xi_{\text{d}}^{\text{max},1} = -Y_{A \rightarrow M_d}^f + c_5 R, \quad (\text{A12a})$$

$$g c_1 P - \beta \left( T_{Af}^1 - M_s \right) + Y_{A \rightarrow M_d}^f - c_5 P = -Y_{A \rightarrow M_d}^f + c_5 P, \quad (\text{A12b})$$

where  $R = \sqrt{\rho_1} \left[ 1 - \exp \left( -d\xi_{\text{d}}^{\text{max},1} \right) \right]$ ,  $P = \sqrt{\rho_1} \times \left[ 1 - \exp \left( -2d\xi_{\text{d}}^{\text{max},1} \right) \right]$ .

In the tenth cycle, the term  $\exp \left( -d \sum_{i=1}^3 \bar{\lambda}_i \right)$  approaches zero, since  $\sum_{i=1}^3 \bar{\lambda}_i$  is a very large number. Thus, the variable  $Z_i$  at the start and finish points, respectively, of the reverse transformation in the tenth cycle can be written as

$$Z_{i,As}^{10} = c_i \sqrt{\rho_{10}}, \quad i = 1, 2, 3, 4, 5, \quad (\text{A13a})$$

$$Z_{i,Af}^{10} = c_i \sqrt{\rho_{10}}, \quad i = 1, 2, 3, 4, 5. \quad (\text{A13b})$$

Similarly, the transformation conditions at the start and finish points of the reverse transformation can be written as:

$$g c_1 \sqrt{\rho_{10}} - \beta \left( T_{As}^{10} - M_s \right) + Y_{A \rightarrow M_d}^f - c_5 \sqrt{\rho_{10}} - \left( H_{A \rightarrow M_d}^f + c_3 \sqrt{\rho_{10}} \right) \xi_{\text{d}}^{\text{max},10} = -Y_{A \rightarrow M_d}^f + c_5 \sqrt{\rho_{10}}, \quad (\text{A14a})$$

$$g c_1 \sqrt{\rho_{10}} - \beta \left( T_{Af}^{10} - M_s \right) + Y_{A \rightarrow M_d}^f - c_5 \sqrt{\rho_{10}} = -Y_{A \rightarrow M_d}^f + c_5 \sqrt{\rho_{10}}. \quad (\text{A14b})$$

After the cyclic deformation, the residual strain  $\varepsilon_r^{10}$  consists of two parts, the transformation strain and the plastic strain, i.e.,

$$\varepsilon_r^{10} = g\xi_d^{M_f,10} + \varepsilon_p^{10}. \quad (\text{A15})$$

By Eq. (A15), the volume fraction of the detwinned martensite phase at the finish point of the forward transformation in the tenth cycle, i.e.,  $\xi_d^{M_f,10}$  can be obtained as

$$\xi_d^{M_f,10} = \frac{\varepsilon_r^{10} - \varepsilon_p^{10}}{g}. \quad (\text{A16})$$

The transformation condition at this point can be written as

$$g c_1 \sqrt{\rho_{10}} - \beta \left( T_{M_f}^{10} - M_s \right) - \left( H_{A \rightarrow M_d}^f + c_3 \sqrt{\rho_{10}} \right) \xi_d^{M_f,10} = 0. \quad (\text{A17})$$

By Eqs. (A12a), (A12b), (A14a), (A14b), and (A17), the five parameters  $H_{A \rightarrow M_d}^f$ ,  $Y_{A \rightarrow M_d}^0$ ,  $c_1$ ,  $c_3$ , and  $c_5$  can be obtained, as shown in Eq. (34f).

In the tenth cycle, the reorientation condition at point  $\sigma_{\text{reo}}^{10}$  can be written as

$$g \left( \sigma_{\text{reo}}^{10} + c_2 \sqrt{\rho_{10}} \right) = Y_{M_t \rightarrow M_d}. \quad (\text{A18})$$

The parameter  $c_2$  can be determined by Eq. (A18), as shown in Eq. (34g).

## References

- Miyazaki, S., Imai, T., Igo, Y., et al.: Effect of cyclic deformation on the pseudoelasticity characteristics of Ti-Ni alloys. *Metall. Trans. A* **17**, 115–120 (1986)
- Song, D., Kang, G., Kan, Q., et al.: Non-proportional multiaxial transformation ratchetting of super-elastic NiTi shape memory alloy: experimental observations. *Mech. Mater.* **70**, 94–105 (2014)
- Song, D., Kang, G., Kan, Q., et al.: Non-proportional multiaxial whole-life transformation ratchetting and fatigue failure of super-elastic NiTi shape memory alloy micro-tubes. *Int. J. Fatigue* **80**, 372–380 (2015)
- Morin, C., Moumni, Z., Zaki, W.: Thermomechanical coupling in shape memory alloys under cyclic loadings: experimental analysis and constitutive modeling. *Int. J. Plast.* **27**, 1959–1980 (2011)
- Kan, Q., Yu, C., Kang, G., et al.: Experimental observations on rate-dependent cyclic deformation of super-elastic NiTi shape memory alloy. *Mech. Mater.* **97**, 48–58 (2016)
- Delville, R., Malard, B., Pilch, J., et al.: Transmission electron microscopy investigation of dislocation slip during superelastic cycling of Ni-Ti wires. *Int. J. Plast.* **27**, 282–297 (2011)
- Kan, Q., Jiang, H., Xu, X., et al.: Experimental observation on thermo-mechanically cyclic deformation of NiTi shape memory alloy. Submitted for publication (2016)
- Huo, Y., Muller, I.: Nonequilibrium thermodynamics of pseudoelasticity. *Continuum Mech. Thermodyn.* **5**, 163–204 (1993)
- Sun, Q.P., He, Y.J.: A multiscale continuum model of the grain-size dependence of the stress hysteresis in shape memory alloy polycrystals. *Int. J. Solids Struct.* **45**, 3868–3896 (2008)
- Dong, L., Sun, Q.P.: On stability of elastic domain during isothermal solid-solid phase transformation in a tube configuration. *Acta Mech. Sinica* **28**, 683–694 (2012)
- Xuan, C., Ding, S., Huo, Y.: Multiple bifurcations and local energy minimizers in thermoelastic martensitic transformations. *Acta Mech. Sinica* **31**, 660–671 (2015)
- Li, J.Y., Lei, C.H., Li, L.J., et al.: Unconventional phase field simulations of transforming materials with evolving microstructures. *Acta Mech. Sinica* **28**, 915–927 (2012)
- Yang, S.Y., Dui, G.S.: Temperature analysis of one-dimensional NiTi shape memory alloys under different loading rates and boundary conditions. *Int. J. Solids Struct.* **50**, 3254–3265 (2013)
- Peng, X., Pi, W., Fan, J.: A microstructure-based constitutive model for the pseudoelastic behavior of NiTi SMAs. *Int. J. Plast.* **24**, 966–990 (2008)
- Lagoudas, D.C., Entchev, P.B.: Modeling of transformation-induced plasticity and its effect on the behavior of porous shape memory alloys. Part I: constitutive model for fully dense SMAs. *Mech. Mater.* **36**, 865–892 (2004)
- Auricchio, F., Reali, A., Stefanelli, U.: A three-dimensional model describing stress-induced solid phase transformation with permanent inelasticity. *Int. J. Plast.* **23**, 207–226 (2007)
- Zaki, W., Moumni, Z.: A 3D model of the cyclic thermomechanical behavior of shape memory alloys. *J. Mech. Phys. Solids* **55**, 2427–2454 (2007)
- Kan, Q., Kang, G.: Constitutive model for uniaxial transformation ratchetting of super-elastic NiTi shape memory alloy at room temperature. *Int. J. Plast.* **26**, 441–465 (2010)
- Yu, C., Kang, G., Kan, Q.: A physical mechanism based constitutive model for temperature-dependent transformation ratchetting of NiTi shape memory alloy: One-dimensional model. *Mech. Mater.* **78**, 1–10 (2014)
- Yu, C., Kang, G., Kan, Q., et al.: Rate-dependent cyclic deformation of super-elastic NiTi shape memory alloy: thermo-mechanical coupled and physical mechanism-based constitutive model. *Int. J. Plast.* **72**, 60–90 (2015)
- Zhang, X., Huang, D., Yan, X., et al.: Modeling functional fatigue of SMA using a more accurate subdivision of martensite volume fractions. *Mech. Mater.* **96**, 12–29 (2016)
- Yu, C., Kang, G., Kan, Q., et al.: Physical mechanism based crystal plasticity model of NiTi shape memory alloy addressing the thermo-mechanical cyclic degeneration of shape memory effect. Under review
- Popov, P., Lagoudas, D.C.: A 3-D constitutive model for shape memory alloys incorporating pseudoelasticity and detwinning of self-accommodated martensite. *Inter. J. Plast.* **23**, 1679–1720 (2007)
- Yu, C., Kang, G., Song, D.: Effect of martensite reorientation and reorientation-induced plasticity on multiaxial transformation ratchetting of super-elastic NiTi shape memory alloy: new consideration in constitutive model. *Int. J. Plast.* **67**, 69–101 (2015)
- Norfleet, D.M., Sarosi, P.M., Manchiraju, S., et al.: Transformation-induced plasticity during pseudoelastic deformation in Ni-Ti microcrystals. *Acta Mater.* **57**, 3549–3561 (2009)
- Simon, T., Kröger, A., Somsen, C., et al.: On the multiplication of dislocations during martensitic transformations in NiTi shape memory alloys. *Acta Mater.* **58**, 1850–1860 (2010)
- Gall, K., Maier, H.J.: Cyclic deformation mechanisms in precipitated NiTi shape memory alloys. *Acta Mater.* **50**, 4643–4657 (2002)
- Wagner, M.F., Nayan, N., Ramamurty, U.: Healing of fatigue damage in NiTi shape memory alloys. *J. Phys. D: Appl. Phys.* **41**, 185408 (2008)

29. Grabe, C., Bruhns, O.T.: On the viscous and strain rate dependent behavior of polycrystalline NiTi. *Int. J. Solids Struct.* **45**, 1876–1895 (2008)
30. He, Y.J., Sun, Q.P.: Frequency-dependent temperature evolution in NiTi shape memory alloy under cyclic loading. *Smart Mater. Struct.* **19**, 115014 (2010)
31. Yin, H., He, Y., Sun, Q.: Effect of deformation frequency on temperature and stress oscillations in cyclic phase transition of NiTi shape memory alloy. *J. Mech. Phys. Solids* **67**, 100–128 (2014)
32. Mecking, H., Kocks, U.F.: Kinetics of flow and strain-hardening. *Acta Metall.* **29**, 1865–1875 (1981)
33. Mareau, C., Favier, V., Weber, B., et al.: Micromechanical modeling of the interactions between the microstructure and the dissipative deformation mechanisms in steels under cyclic loading. *Int. J. Plast.* **32**, 106–120 (2012)
34. Otsuka, K., Ren, X., et al.: Physical metallurgy of Ti-Ni-based shape memory alloys. *Prog. Mater. Sci* **50**, 511–678 (2005)